J Mater Sci (2010) 45:5778–5785
DOI 10.1007/s10853-010-4651-9

Bimodal cellular activated carbons derived from tannins

W. Zhao · V. Fierro · A. Pizzi · A. Celzard

Received: 7 March 2010 / Accepted: 21 May 2010 / Published online: 4 June 2010

Abstract New cellular activated carbons mainly derived from tannins and furfuryl alcohol are introduced and suggested as adsorbents and catalyst supports. They present a bimodal porosity, based on a highly porous, reticulated vitreous carbon backbone, whose micro/meso-porosity was developed by steam activation. The macroporosity corresponds to the connected network of cells whose average diameter is close to 250 μm. In contrast, the micro/meso-porosity is located at the inner surface of the cells and is thus fully and easily accessible. Consequently, much higher adsorption kinetics than for usual granular activated carbons are expected. A burn-off close to 30% was shown to be optimal for getting a high proportion of microporosity without complete loss of mechanical resistance. In these conditions, the surface area is close to 850 $m^2\ g^{-1}$, thus similar to that of many commercial carbonaceous adsorbents.

Introduction

Activated carbons (ACs) are materials of key importance for industrial applications. Their outstandingly high surface area gives them irreplaceable adsorption properties for pollutant removal in the liquid or in the gas phase [1]. They are also valuable catalyst supports, allowing an excellent dispersion of nanoparticles [2]. Moreover, in the latter application, carbon may be burnt at the end of the catalyst shelf life in order to recover the precious metals. Other kinds of catalysts based on carbide nanoparticles were also shown to be advantageously prepared by reaction with the carbon support itself [3].

In all these applications, adsorption or catalysis, fast availability of active sites is required. Most of times, commercial ACs are in the form of grains whose surface area is mainly controlled by their inner microporosity (pore widths $w < 2$ nm [4]). Mesopores ($2 < w < 50$ nm [4]) are pathways for reactants flowing throughout carbon grains, but mesoporosity is highly tortuous and its corresponding volume may not be high enough. Consequently, adsorption kinetics are usually slow, thus reducing the efficiency of dynamical adsorption or catalytic processes [5, 6].

Taking into account the aforementioned considerations, a bimodal cellular activated carbon was developed in the present work. This material is composed at the 95% level of natural resources: tannins and furfuryl alcohol. Tannins are polyfavonoids extracted from barks [7]. Furfuryl alcohol is obtained from the catalytic reduction of furfural, a natural derivative obtained by hydrolysis of the sugars from several agricultural crops [8]. Advantages of such a cellular carbon is its renewable origin and low cost. The cost of the raw carbon foam before activation is indeed lower than 10 US $ per kg, i.e. it is the cheapest carbon foam among those presently commercialised [9]. The cellular activated carbon presented here is based on such open-celled carbon foam, whose inner surface was activated in order to present a fully available surface micro/meso-porosity. Given its high permeability, from 5 to 50 Darcy [10], it is expected that dynamical processes

W. Zhao · V. Fierro · A. Celzard (✉)
Département 2: Chimie et Physique des Solides et des Surfaces, Institut Jean Lamour, UMR 7198, CNRS – Nancy-Université – UPV-Metz, ENSTIB, 27 rue du Merle Blanc, BP 1041, 88051 Epinal Cedex 9, France
e-mail: Alain.Celzard@enstib.uhp-nancy.fr

A. Pizzi
ENSTIB – LERMAB, 27 rue du Merle Blanc, BP 1041, 88051 Epinal Cedex 9, France

occurring in the porosity can be achieved at much higher rates than in any granular AC of similar surface area.

A bimodal activated carbon having its micro- and mesoporosity mostly located at the surface of much wider, fully connected macropores is expected to have the same applications as classical ACs. Examples are adsorption of hazardous or valuable chemicals (heavy metals, pesticides, dyes or pharmaceuticals). However, the key feature of this new material is expected to be its much higher adsorption kinetics related to its unique pore structure. Detailed adsorption experiments will be the purpose of a forthcoming article.

Preparation of bimodal cellular ACs derived from tannin-based carbon foam is described in "Experimental" section, wherein characterisation methods are described as well. "Results and discussion" section gathers results of pore texture analysis and related mechanical properties.

Experimental

Preparation of cellular ACs derived from tannins

Preparation of RVC foam

The precursor of the ACs introduced here is a reticulated vitreous carbon (RVC) foam derived from tannins. Its preparation has been presented elsewhere in detail [9] and is only briefly recalled here.

5.2 g of furfuryl alcohol, 3.7 g formaldehyde (37% water solution) and 3.0 g of water were mixed with 15 g of spray-dried powder of Mimosa tannin extract (from SilvaChimica, Italy), strongly stirring the bulk. When the agglomerate was homogeneous, 1.5 g of diethylether and then 6.0 g of toluene-4-sulphonic acid (65% water solution) were added and sufficiently mixed for 10 s before discharging into a lined box for foaming. Due to the heat generated by the polymerisation of tannin and furfuryl alcohol, boiling of diethylether occurred, so that the resin foamed within 2 min of mixing. Black rigid foam was obtained and left to harden and age for a few days.

The external parts of the organic foam (over a thickness of a few millimetres beneath the skin) were systematically eliminated. Cubic pieces (typical side 2 cm) were cut off with a knife for subsequent pyrolysis. Carbonisation of the samples was carried out inside a quartz tube continuously flushed with high-purity nitrogen. The tube was heated by an electric furnace from room temperature up to 900 °C at 4 °C min^{-1}. Once reached, the final temperature was held for 2 h, then the furnace was switched off, and the samples were allowed to cool down to room temperature under nitrogen flow. Black, shiny, cubic RVC foam samples were thus recovered.

The foam being grown vertically, the cells were slightly elongated along the vertical direction, here referred to as z. Anisotropy was thus expected and was indeed already evidenced [10, 11]. Consequently, in the following, mechanical properties have been measured along z and along the horizontal plane here called the xy direction.

Preparation of cellular activated carbons

Because of their thin pore walls, activation of such carbon foams was not carried out directly; otherwise extremely low mechanical properties would be obtained [12]. The backbone of RVC foams was then thickened through impregnation by furfuryl alcohol followed by carbonisation. For that purpose, the samples were immersed in furfuryl alcohol and submitted to three vacuum-atmospheric pressure cycles, in order to intrude thoroughly the porosity. The samples were then drained on a metal grid, and the furfuryl alcohol remaining inside was polymerised by soaking the samples in 0.5 N HCl aqueous solution during 5 h. Next, the materials were dried in air at room temperature (12 h), then in an oven whose temperature was gradually increased (3 °C min^{-1}) until the final set point, 120 °C, was reached and maintained overnight. Finally, the samples were carbonised at 550 °C (4 °C min^{-1}) in a tubular quartz reactor and continuously flushed with high purity nitrogen.

The resultant-coated samples were thus activated with steam in a tilted quartz tube heated at 800 °C. A pump injected water at 0.5 mL min^{-1} inside the tube which vaporised immediately inside and was carried out by nitrogen flowing at 50 mL min^{-1}. Depending on the duration of the experiment, various burn-offs, defined as the percents of weight loss, were obtained.

Characterisation of the ACs

Surface area and porosity

Nitrogen adsorption isotherms were obtained at 77 K using a Micromeritics ASAP 2020 automatic adsorption apparatus. The samples were outgassed for 48 h under vacuum at 523 K prior to any adsorption experiment.

In order to obtain "high resolution" adsorption isotherms, adsorbed volumes of nitrogen were measured at relative pressures P/P_0 as low as 10^{-7}. Adsorption isotherms were determined by dosing nitrogen volumes of 25 STP cm^3 g^{-1} up to $P/P_0 = 10^{-6}$, whereas a table of relative pressures was used to build the isotherms up to a final P/P_0 of 0.99. Surface areas, S_{BET}, were determined by the BET calculation method [13] applied to the adsorption branch of the isotherms. The micropore volume, V_{DR} was determined according to the Dubinin–Radushkevich (DR)

method ([14] and refs. therein), with correlation coefficients equal to or higher than 0.999. The total pore volume, sometimes referred to as the Gurvitch volume, $V_{0.99}$, was defined as the volume of liquid nitrogen corresponding to the amount adsorbed at a relative pressure $P/P_0 = 0.99$ [15]. The average micropore diameter, L_0, was calculated from the following expression [16]:

$$L_0 = \frac{10.8\ (\text{nm kJ mol}^{-1})}{E_0 - 11.4\ (\text{kJ mol}^{-1})}. \quad (1)$$

In Eq. 1, E_0 is the characteristic adsorption energy of nitrogen and was derived from the corresponding adsorption isotherms at 77 K, applying the DR method.

Finally, the micro/meso-pore size distributions were calculated by application of the DFT model [17] supplied by Micromeritics software, considering slit-shaped pores.

Total porosity of the materials, P, was defined as:

$$P = 1 - \frac{d}{d_s}, \quad (2)$$

where d is the bulk density of the foams and d_s the skeletal density. d is defined as the mass of material divided by the total volume it occupies and is measured by weighing a number of parallelepiped samples of known dimensions. d_s has been determined elsewhere [18] by helium pycnometry in a lab-made apparatus.

Mechanical properties

Complete stress–strain compression characteristics were recorded with an Instron 4206 universal testing machine equipped with a 1-kN head and using a load rate of 2.0 mm min^{-1}. One sample of typical dimensions 1.5 × 1.5 × 1.5 cm was used for each of the two measurement directions xy and z considered here.

All stress–strain curves presented three distinct regions (see next section): linear elastic at low stresses and up to 10% strain, on average, collapse and densification. In the first zone of elastic deformation, discontinuities indicated the rupture of the weakest individual elements of the material: protruding struts and cell edges. The subsequent, long, serrated plateau, usually ranging from 10 to 80% strain, originated from the co-existence of collapsed and uncollapsed zones. This feature is typical of brittle foam undergoing successive and propagating cell wall fractures. The "noisy" aspect of the curve was due to the redistribution of the compression after the fracture of some layers of cells, followed by the loading of the subsequent cell layers. The fracture strength thus did not depend on the strain, like in most nonporous materials. Beyond the plateau, densification took place when all the cell bands had collapsed. The stress thus rose sharply with further strain.

Young's modulus was defined as the slope of the linear, initial, part of the curve presenting the steepest slope [19]. The very beginning of the curve indeed corresponded to the parallelization of the opposite surfaces submitted to compressive stress, and thus presented several irregularities. In the second plateau region, the maximum stress was recorded and referred to as the maximum compressive strength.

Results and discussion

Density and porosity of RVC foams and derived ACs

Raw and coated RVC foams

According to the formulation given in "Preparation of RVC foam" section, organic foam samples having a bulk density close to 0.07 g cm^{-3} were obtained. Pyrolysis at 900 °C produced almost no change of bulk density, given that the shrinkage that occurred during carbonisation was exactly compensated by weight loss, as already demonstrated elsewhere [9, 18]. According to Eq. 2 and given the skeletal density of RVC carbon, 1.98 g cm^{-3} [18], the porosity of raw RVC foams was 96.5%.

The bulk density of 20 samples of RVC foams before and after impregnation by polymerised, dried, furfuryl alcohol and after subsequent carbonisation is presented in Fig. 1. The reproducibility of the results is satisfactory, despite density fluctuations due to difficulties of preparing strictly identical samples. The bulk density rose from 0.07 to 0.5 g cm^{-3}, on average, through the impregnation process. Given the density of polymerised furfuryl alcohol (PFA), 1.25 g cm^{-3} [20], 0.344 cm^3 of PFA was

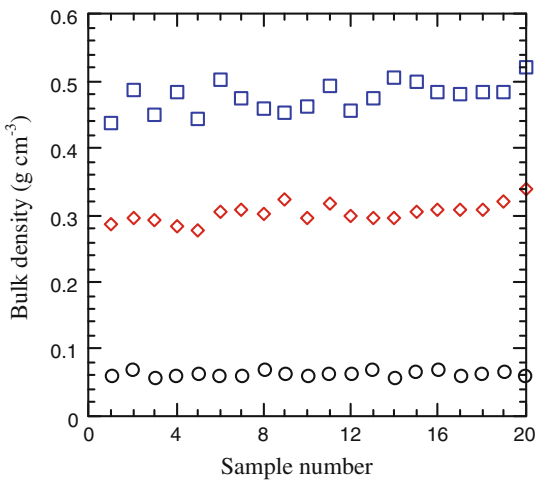

Fig. 1 Bulk density of 20 samples of RVC foam: (*open circle*) before and (*open square*) after impregnation with furfuryl alcohol and (*open diamond*) after subsequent pyrolysis

introduced in the porosity of 1 cm^3 of initial RVC foam. In other words, 36% of the foam's porosity has been filled with PFA. The surface area of raw RVC foam has been measured by nitrogen adsorption at 77 K and found to be 0.89 $m^2\ g^{-1}$ [9]. Assuming that PFA homogeneously coated the inner surface of the cells, the average thickness of PFA could be calculated and found to be $0.344/(0.89 \times 0.07) = 5.5$ μm.

After pyrolysis, the bulk density of the samples was decreased to 0.3 g cm^{-3}, on average, indicating a coke yield close to 53%. This value is between those obtained elsewhere with different heating rates: 60% at 3 °C min^{-1} [20], on one hand, and 40% at 10 °C min^{-1} [21], on the other hand. The skeletal density of glasslike carbon derived from the pyrolysis of PFA is 1.45 g cm^{-3} [21], from which the thickness of the coating of coke deposited in the porosity of RVC foam was calculated as above, 2.5 μm. Such a value is far below the average diameters of both cells and cell windows: 250 and 60 μm, respectively [18]. Consequently, physical properties related to the pore space, tortuosity, permeability, diffusion in the pore space, are not supposed to be seriously affected by the inner coating of coke. However, the latter is expected to improve the mechanical behaviour of the cellular material and to be sufficiently thick for being the source of micro/meso-porosity by steam activation.

Activated coated RVC foams

Steam activation is a controlled gasification of carbonaceous materials, leading to micro or mesopores, depending on the duration of the experiment. Burn-off was found to increase linearly with activation time (not shown). A maximum burn-off close to 50% was considered here because of the corresponding dramatic loss of mechanical properties (see below).

A few of the corresponding nitrogen adsorption–desorption isotherms are presented in Fig. 2a; all are of type I according to the IUPAC classification [4]. These isotherms are characteristic of microporous materials and present a sharp increase of N_2 adsorbed volume at very low relative pressures, an almost horizontal plateau and a very narrow adsorption–desorption hysteresis cycle. The latter broadens with the burn-off but remains rather flat, indicating that the mesopore volume is low. Most of these cellular ACs thus mainly have a microporous character. Increasing the burn-off made the knee of the isotherm become wider, which is related to a broadening of micropore width. This effect is best demonstrated in Fig. 2b, presenting the same data on a logarithmic scale: widening of the isotherm knee and increasing of the slope are clearly seen.

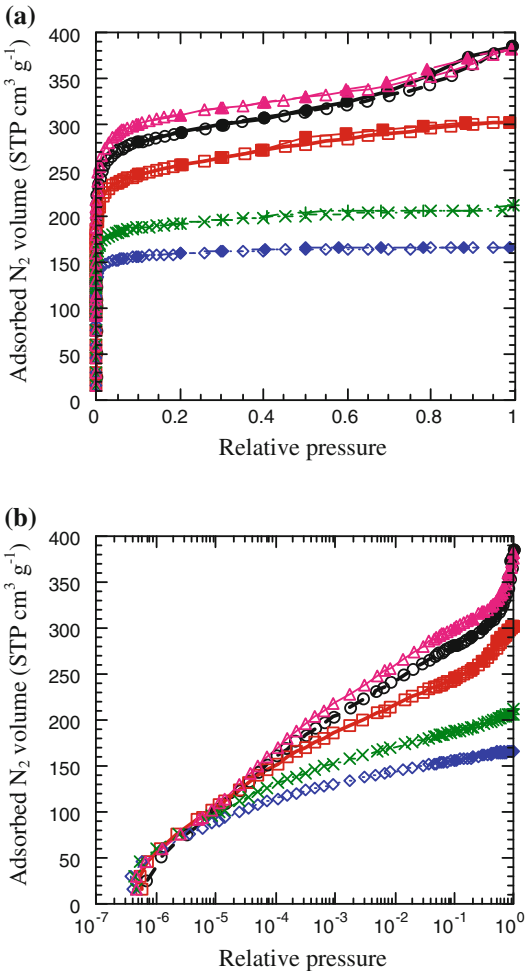

Fig. 2 N_2 isotherms at 77 K of a few steam activated, coated, RVC foams, as a function of relative pressure: **a** adsorption–desorption isotherms in linear scale; **b** adsorption in logarithmic scale. Full and open symbols stand for adsorption and desorption, respectively. Burn-offs are (*open diamond*) 15.3%; (*times*) 25%; (*open square*) 35.3%; (*open circle*) 52.6%; (*open triangle*) 53%

Figure 3 shows pore-size distribution (PSD) derived from Fig. 2a and corroborates the aforementioned findings. Higher burn-offs correspond to both broadened microporosity and to a dramatic decrease of the number of pores narrower than 0.7 nm. Low burn-offs lead to very narrow PSD centred on very narrow micropores, but also to low pore volumes. A compromise between narrow microporosity and high micropore volume seems to occur near 35% burn-off, at which the surface area is close to 1000 $m^2\ g^{-1}$ (see next Fig. 4). Such a value is typical of most commercial ACs.

BET surface areas calculated from Fig. 2a are plotted in Fig. 4a as a function of burn-off. In the considered range of burn-offs, a linear correlation was found between surface area and weight loss. It is then very easy to control the development of the porosity of coated RVC foams. The same was observed in Fig. 4b, in which the different pore

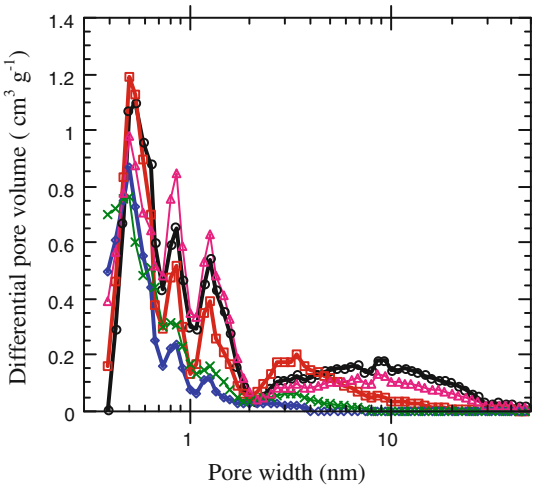

Fig. 3 Pore-size distributions calculated from Fig. 2a, using the DFT model. The symbols standing for the burn-offs are the same as in Fig. 2

volumes that have been created by the activation process, micropores (V_{DR}), mesopores (V_{meso}) and total ($V_{0.99}$), are plotted as a function of burn-off. Again, a straight line could be drawn for describing the behaviour of each quantity. As already revealed by the adsorption isotherms given in Fig. 2a, microporosity and mesoporosity were simultaneously developed as the burn-off increased. This finding was expected, given that physical activation is a gasification, hence a process that creates small pores but also broadens already existing pores without selectivity.

An alternative way of observing this phenomenon is given in Fig. 4c, in which the average micropore with L_0 calculated from Eq. 1 is plotted as a function of burn-off. In agreement with the PSD of Fig. 3, the microporosity was broadened when the burn-off increased. Once more, a linear correlation was observed.

Bimodal character of the porosity of activated coated RVC foams

The major interest of preparing an AC from a cellular carbon is based on the bimodal character of the resultant porosity: a broad, macroscopic, fully connected porosity, on one hand, and a narrow, nanometric surface microporosity, on the other hand. The former confers a high permeability to the material and a fast access to the microporosity, whereas the latter provides active sites for adsorption or even for catalysis if nanoparticles have been dispersed beforehand. The relative proportions of each kind of porosity are now determined.

The pore volumes created by activation, expressed in cm^3 g^{-1}, have been given in Fig. 4b. The mass of each activated foam and hence its absolute micro/meso-pore volume could be calculated from the known corresponding

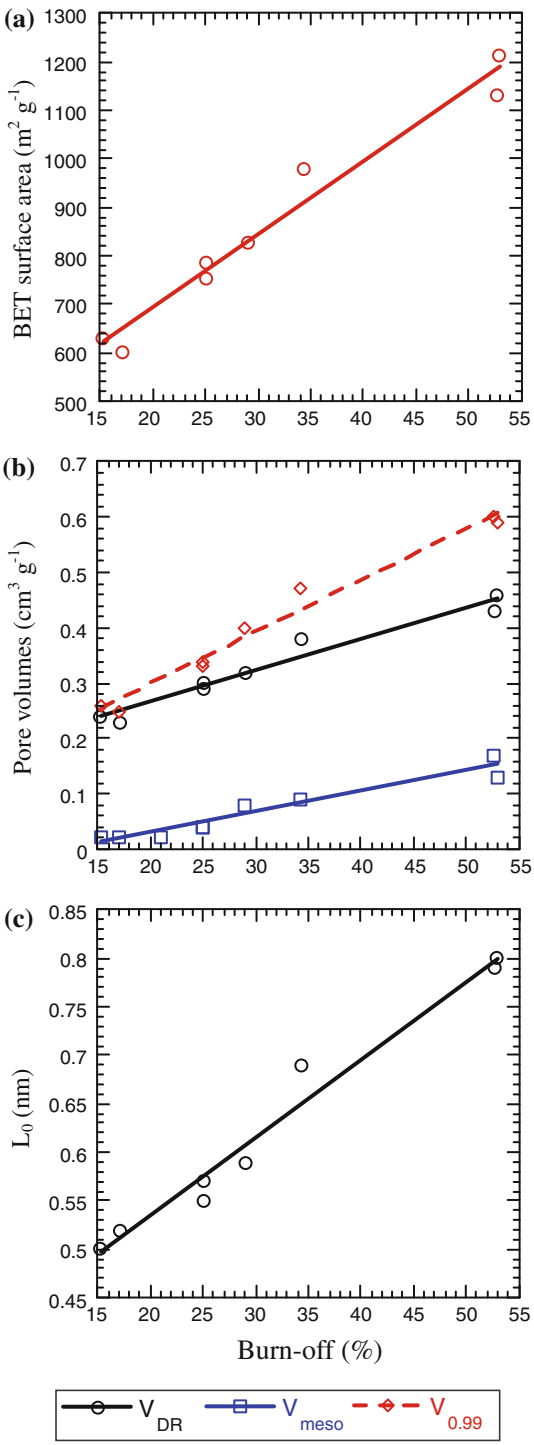

Fig. 4 Pore texture characteristics of activated, coated, RVC foams as a function of burn-off: **a** BET surface area; **b** pore volumes generated by activation; and **c** average micropore width

burn-offs. Given the bulk densities of initial RVC foam and impregnated foam after carbonisation (0.07 and 0.3, respectively) and the skeletal densities of RVC and furfuryl alcohol char (1.98 and 1.45, respectively), the porosity of the material before activation was found to be 80.6%. Such

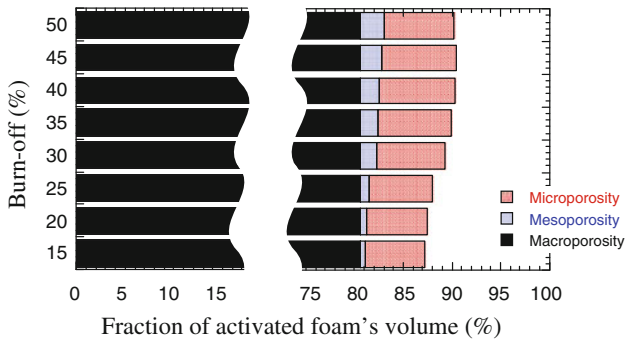

Fig. 5 Volume fractions of cellular activated carbons, separated according to the width of the porosity: macroporosity (interconnected cell space), surface mesoporosity (pore widths below 50 nm and above 2 nm) and surface microporosity (pore widths below 2 nm). The remainder corresponds to the solid phase

a macroporosity should not change during activation, since only the carbon coating derived from the pyrolysis of furfuryl alcohol is expected to be progressively gasified. This rough assumption is justified by the fact that the maximum burn-off investigated here is 50%, whereas the weight of the furfuryl alcohol char is typically four times higher than that of the original carbon foam (see Fig. 1). In other words, the coating is much thicker than the original foam backbone and is thus expected to be first and foremost gasified. The different calculated proportions of the total porosity are presented in Fig. 5.

The bimodal character of the porosity is clearly evidenced, for which typically 80% of the foam volume corresponds to macropores having diameters close to 250 μm and up to 10% are surface pores having widths below 50 nm. It can be seen that the percentage of microporosity reached a maximum at a burn-off of 35–40%, whereas the mesoporosity always increased with burn-off. Even if burn-offs beyond 40% weight loss led to higher surface area, as demonstrated by Fig. 4a, a more advanced activation decreased the microporous character of the material and also lessened its mechanical resistance, as detailed below.

Mechanical properties of RVC foams and derived ACs

Stress–strain characteristics

The stress–strain curves of raw and coated RVC foams, i.e. having densities of 0.07 and 0.3 g cm^{-3}, respectively, are given in Fig. 6a. The three typical zones of the graph, described in "Characterisation of ACs" section, were clearly identified. Raw RVC foams presented higher compressive strength along *z*-axis, probably because the struts are preferentially oriented along this direction. After deposition of glasslike carbon inside the cells, anisotropy was considerably decreased, given that the plateau stresses

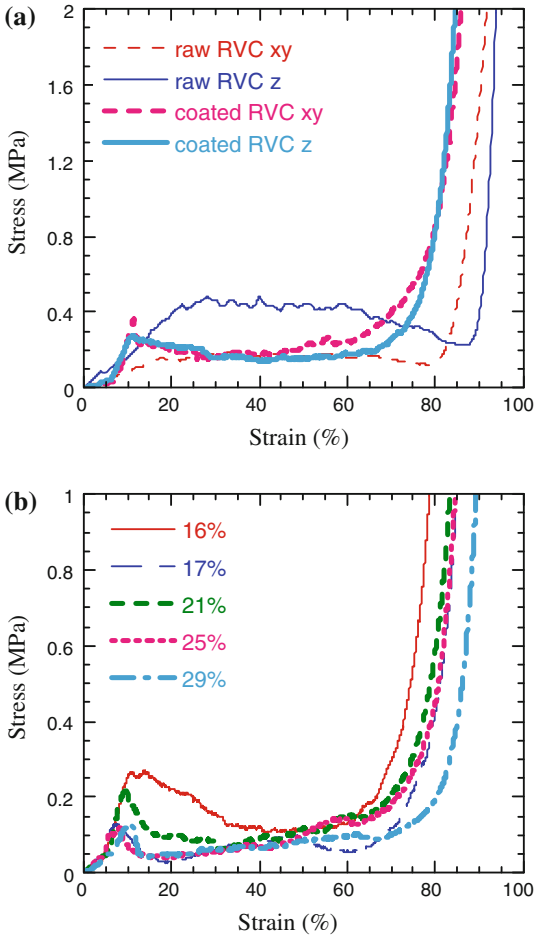

Fig. 6 Stress–strain characteristics of: **a** raw and coated RVC foams; **b** activated coated foams measured along *z*-axis. The burn-off (%) is indicated on the graph

along *xy*- and *z*-axes were observed at similar stresses. Coating RVC foams thus made the cellular carbons more homogeneous. Surprisingly, after this process, the compressive strength was not increased, suggesting that the deposited carbon had a brittle nature, just like the one constituting the raw RVC foams. In contrast, elastic modulus was significantly enhanced. As expected, compression-induced densification occurred at lower strain, typically 70–80% after deposition of glasslike carbon within the cells, instead of 80–90% for raw RVC foams.

Stress–strain curves of activated coated foams measured along *z*-axis (measurements along *xy*-axes are not shown) are presented in Fig. 6b. No burn-off higher than 30% was investigated for its mechanical properties because highly activated materials were very friable, and a significant lack of accuracy was expected with the available testing machine. The same general behaviour with its three successive zones, linear elastic, collapse and densification, was fully maintained after activation, whatever the burn-off. As expected, both elastic modulus and compressive strength

decreased with burn-off, on average, whereas densification strain increased.

Elastic modulus

Elastic moduli derived from Fig. 6 are presented in Fig. 7a. Deposition of glasslike carbon inside the cells of RVC foams multiplied the elastic modulus by a factor 3. However, the elastic modulus was considerably decreased by activation, even at low burn-off. A linear trend was evidenced, despite the natural scattering of the data due to the slightly different densities of the foams before activation. The fitted straight line had a similar slope for each measurement direction and suggested that the elastic modulus vanished for a burn-off of 34 and 37% along *xy* and *z* directions, respectively. These values underestimate the maximum possible burn-off, given that consolidated materials have been experimentally obtained with burn-offs higher than 50%. However, it is true that the mechanical resistance of such materials was very low, so even if the modulus was not zero, it was very small indeed.

Maximum compressive strength

Figure 7b presents the maximum compressive strengths derived from the curves of Fig. 6. Just like for elastic modulus, a linear decrease was evidenced as a function of burn-off. The slope was more or less the same for both measurement directions, and the mechanical resistance was found to vanish for burn-offs of 38 and 42% along *xy* and *z*, respectively. These values are again underestimated, but suggest that burn-offs higher than 40% lead to very weak materials, i.e. not suitable for industrial applications such as adsorption or catalysis in the form of monoliths. It seems that burn-offs higher than 30% should not be used, except if the materials can be used in the form of powder.

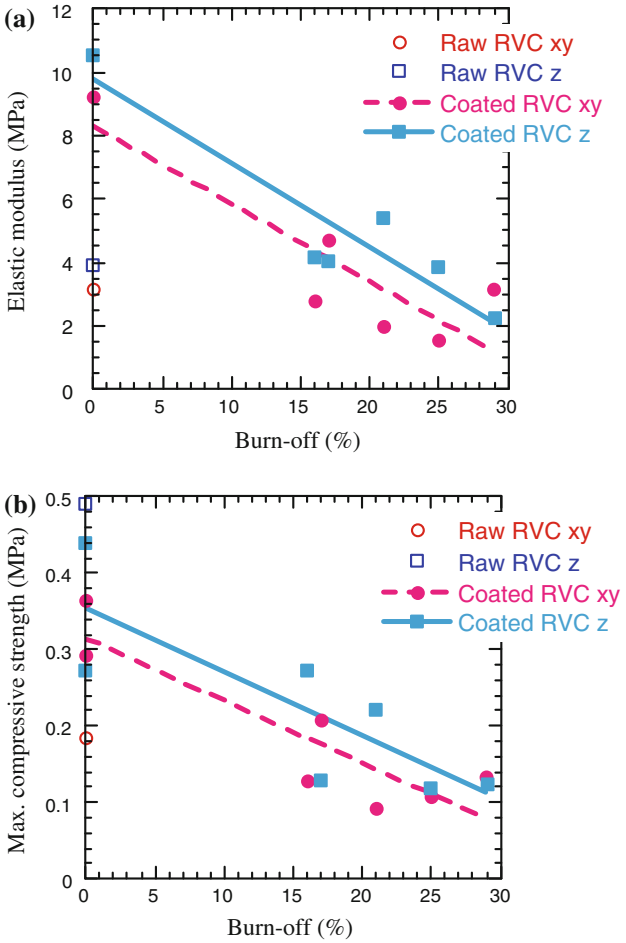

Fig. 7 Mechanical properties of raw, coated and activated RVC foams as a function of burn-off: **a** elastic modulus; **b** maximum compressive strength

Conclusions

In the present work, new cellular activated carbons have been presented. They are based on a backbone of RVC mainly derived from vegetable extracts (tannins), which was next coated by glasslike carbon derived from furfuryl alcohol. The porosity of such cellular materials presented a bimodal character, since comprising a wide, fully connected network of cells of diameter close to 250 μm, at the surface of which micro/meso-porosity has been created by steam activation.

A burn-off close to 30% seemed to be an optimum for getting valuable adsorption performances without complete loss of mechanical properties. The results presented in this paper indeed showed that such a burn-off led to a compromise between narrow microporosity and high micropore volume, on one hand, and to a high percentage of microporosity, on the other hand. Moreover, higher burn-offs seriously degraded the mechanical properties, possibly destroying the monolithic nature of the AC. The corresponding surface area was close to 850 $m^2\ g^{-1}$, typical of a number of commercial ACs.

However, unlike usual adsorbents, the micro/meso-porosity is fully accessible to any pollutant to be removed or to any reagent to be catalytically converted at the carbon surface. No diffusion limitation should exist, so these new cellular activated carbons should present extremely high adsorption or catalysis kinetics. If their monolithic shape is maintained, permeabilities as high as 50 Da are expected. The materials could also be used in powder form, even enhancing the ultra-fast availability of the surface micro/meso-porosity. Experiments for measuring adsorption kinetics of tannin-based cellular adsorbents, with comparison with granular and powdery ACs of similar pore textures and surface areas, are currently in progress.

Acknowledgements The authors gratefully acknowledge the financial support of the CPER 2007-2013 "Structuration du Pôle de Compétitivité Fibres Grand'Est" (Competitiveness Fibre Cluster), through local (Conseil Général des Vosges), regional (Région Lorraine), national (DRRT and FNADT) and European (FEDER) funds.

References

1. Świątkowski A (1999) Stud Surf Sci Catal 120:69
2. Rodríguez-Reinoso F, Sepúlveda-Escribano A (2001) In: Nalwa HS (ed) Adsorption and catalysis, handbook of surfaces and interfaces of materials. Academic Press, San Diego
3. Celzard A, Marêché JF, Furdin G, Fierro V, Sayag C, Pielaszek J (2005) Green Chem 7:784
4. Sing KSW, Everett DH, Haul RAW, Moscou L, Pierotti RA, Rouquerol J, Siemieniewska T (1985) Pure Appl Chem 57:603
5. Hu X, Do DD (1993) Chem Eng Sci 48:1317
6. Scholl S, Kajszika H, Mersmann A (1993) Gas Sep Purif 7:207
7. Meikleham NE, Pizzi A (1994) J Appl Polym Sci 53:1547
8. Aguilar R, Ramırez JA, Garrote G, Vazque M (2002) J Food Eng 55:309
9. Tondi G, Fierro V, Pizzi A, Celzard A (2009) Carbon 47:1480
10. Zhao W, Fierro V, Pizzi A, Du G, Celzard A (2010) Mater Chem Phys. doi:10.1016/j.matchemphys.2010.03.084
11. Tondi G, Zhao W, Pizzi A, Du G, Fierro V, Celzard A (2009) Biores Technol 100:5162
12. Tondi G (2009) PhD Thesis, University of Nancy I, ENSTIB
13. Brunauer S, Emmet PH, Teller E (1938) J Am Chem Soc 60:309
14. Dubinin MM (1989) Carbon 27:457
15. Gregg SJ, Sing KSW (1982) Adsorption, surface area and porosity, 2nd edn. Academic Press, London
16. Stoeckli F, Slasli A, Hugi-Cleary D, Guillot A (2002) Microporous Mesoporous Mater 51:197
17. Tarazona P (1995) Surf Sci 331–333:989
18. Zhao W, Pizzi A, Fierro V, Du G, Celzard A (2010) Mater Chem Phys 122:175
19. Celzard A, Zhao W, Pizzi A, Fierro V (2010) Mater Sci Eng A 527:4438
20. Celzard A, Krzesinska M, Bégin D, Marêché JF, Puricelli S, Furdin G (2002) Carbon 40:557
21. Burket CL, Rajagopalan R, Marencic AP, Dronvajjala K, Foley HC (2006) Carbon 44:2957